

Influence of e - e scattering on the temperature dependence of the resistance of a ballistic point-contact in a 2DES

M.Yu. Melnikov,¹ J.P. Kotthaus,² V. Pellegrini,³ L. Sorba,³ G. Biasiol,⁴ and V.S. Khrapai¹

¹*Institute of Solid State Physics, Russian Academy of Sciences, 142432 Chernogolovka, Russian Federation*

²*Center for NanoScience and Fakultät für Physik, Ludwig-Maximilians-Universität, Geschwister-Scholl-Platz 1, D-80539 München, Germany*

³*NEST, Istituto Nanoscienze-CNR and Scuola Normale Superiore, Piazza San Silvestro 12, I-56127 Pisa, Italy*

⁴*CNR-IOM, Laboratorio TASC, Area Science Park, I-34149 Trieste, Italy*

We experimentally investigate the temperature (T) dependence of the resistance of a ballistic point contact (PC) in a two-dimensional electron system (2DES). The split-gate PC is realized in a high-quality AlGaAs/GaAs heterostructure. The PC resistance is found to drop by more than 10% as the T is raised from 0.5K to 4.2 K. In the absence of magnetic field, the T -dependence is roughly linear below 2K, and tends to saturate at higher T . Perpendicular magnetic fields on the order of a few 10mT suppress the T -dependent contribution δR . This effect is more pronounced at lower temperatures, causing a crossover to a nearly parabolic T -dependence in magnetic field. The normalized magnetic field dependencies $\delta R(B)$ permit an empiric single parameter scaling in a wide range of PC gate voltages. These observations give strong evidence for the influence of electron-electron (e - e) scattering on the resistance of ballistic PCs. Our results are in qualitative agreement with a recent theory of the e - e scattering based T -dependence of the conductance of classical ballistic PCs [Phys. Rev. Lett. **101**, 216807 (2008)] and [Phys. Rev. B **81**, 125316 (2010)].

I. INTRODUCTION

Electronic conductance of a diffusive solid-state system is characterized by a mean-free path of charge carriers (l_0). Scattering processes off disorder and phonons, as well as electron-electron scattering (via U-processes), contribute a total quasi-momentum relaxation rate, inversely proportional to l_0 . At increasing temperature (T) the scattering typically becomes more effective and the mean-free path decreases. The impact of scattering on the T -dependence of the conductance is different in ballistic systems, among which a point contact is, perhaps, the simplest.

Introduced by Sharvin¹, a classical ballistic point contact (PC) is represented by an orifice between two clean reservoirs with dimensions large compared to the inverse Fermi-momentum (k_F). In two-dimensions (2D), the conductance of the classical PC is given by a well-known analogue of the Sharvin formula²:

$$G_0 = \frac{2e^2}{\hbar} \frac{ak_F}{\pi^2}, \quad (1)$$

where e is the elementary charge, \hbar is the Planck constant and a is a half-width of the PC orifice, $ak_F \gg 1$. Finite mean-free path in the reservoirs gives rise to a nonzero backscattering probability of carriers injected through the PC. As a result, the PC conductance is smaller than the ideal value (1) roughly by $\delta G/G_0 \sim -a/l_0$. At increasing T the mean-free path l_0 decreases and causes a negative T -dependence of the PC conductance. Sizeable in disordered systems, this effect can be neglected in contemporary high quality devices ($a/l_0 \sim 1\%$) including those studied here.

In a recent work¹³, impact of the e - e scattering on the conductance of classical PCs has been analyzed. As shown by authors, the dominant contribution comes from

scattering of injected electrons with those incident onto the PC at large distances from the orifice. Contrary to naive expectations, this scattering mechanism *enhances* the conductance of the PC. For a classical PC in a two-dimensional electron system (2DES) with Fermi energy E_F and temperature T the e - e scattering contribution is found to be (the numerical factor is given after¹⁵):

$$\frac{\delta G_{ee}}{G_0} \approx 0.037 \alpha_{ee} (ak_F) \frac{k_B T}{E_F} \ln(l_c/a), \quad (2)$$

where $\alpha_{ee} \sim 1$ is a dimensionless e - e interaction parameter, k_B is the Boltzman constant and $l_c \sim l_0 \gg a$ is a cutoff length-scale in the 2DES. For a typical PC in a 2DES in GaAs the e - e scattering contribution is estimated as $\sim 10\%$ at liquid He temperatures and hence expected to dominate the T -dependence. More recently¹⁴, a suppression of the e - e scattering contribution to the PC conductance in small perpendicular magnetic fields has been calculated.

Ballistic constrictions in 2D have been extensively studied since the first observations of conductance quantization^{3,4}. Thermal smearing of the conductance plateaus causes a well known T -dependence mechanism in such devices^{5,6}. Quantum-dot-Kondo-like T -dependence in the region of the so-called 0.7 anomaly⁷ is associated with many-body physics. E-e scattering-induced size effects in wide and long quasiballistic channels have been studied in⁸. In those experiments, a current self-heating was used to vary the electronic temperature and a non-monotonic behavior of the differential resistance was observed. The results were later interpreted as a 2D analogue of a hydrodynamic-like Gurzhi effect⁹. A non-local hydrodynamic-like problem of electron injection through a PC was addressed in¹⁰ in case of e - e scattering dominating all other scattering mechanisms. Corresponding experiments¹¹ have been per-

formed in wide channels in a strongly nonlinear regime. Observation of the e - e scattering contribution to the linear response Sharvin conductance requires careful measurements of the T -dependence and magnetoresistance in PCs formed in a clean 2DES. We are aware of only one such experiment¹², which is qualitatively consistent with the e - e scattering scenario of Refs.^{13,14}.

Here we present an experimental study of a T -dependence of the resistance in split-gate defined PCs in a GaAs-based 2DES at liquid He temperatures. In the absence of magnetic field, the negative T -dependent resistance contribution on the order of 10% is found. The T -dependence is suppressed by a small perpendicular magnetic field of a few 10mT. The normalized magnetic field dependencies for different gate-voltages obey an empiric single-parameter scaling procedure. The results give strong evidence for the influence of the e - e scattering on the PC conductance and are qualitatively consistent with the predictions of Refs.^{13,14}. We compare the measured functional dependencies on temperature and magnetic field with the theory predictions and discuss possible origins of the discrepancies, supporting by a numerical calculation. In the absence of a magnetic field a rough quantitative agreement is achieved and the interaction parameter α_{ee} is evaluated.

The paper is organized as follows. The experimental details are described in section II. The results in zero and finite magnetic field are presented in sections III and IV, respectively. Section V is devoted to scaling of the magnetoresistance data. The discussion of the experimental results is given in section VI. The details of evaluation of the electron density inside the PC and those of numerical calculation are given in Appendix. The paper is briefly summarized in section VII.

II. EXPERIMENTAL DETAILS

Our samples are based on a high quality (001)GaAs/AlGaAs heterostructure containing a 2DES 200nm below the surface. The electron density is about $n_S \approx 0.83 \cdot 10^{11} \text{cm}^{-2}$ and the mobility is $\approx 4 \cdot 10^6 \text{cm}^2/\text{Vs}$ at $T = 4.2\text{K}$, which corresponds to an elastic mean free path of $\approx 20\mu\text{m}$. The inset of fig. 1 shows a micrograph of metallic split gates deposited on the crystal surface with the help of e-beam lithography (shown as two brighter areas). Negative gate voltages are applied to the gates in order to deplete the 2DES beneath them and define a PC. Throughout the paper, the voltage on the right gate is fixed at -0.4V , while the left gate voltage (below simply gate voltage, V_g) can be varied to control resistance of the PC. The ohmic contacts to the electron system are obtained via annealing of Ni/Au/Ge/Ni/Au and situated at distances about 1mm away from the PC. The experiment is performed in a ^3He insert at temperatures between 0.46 and 4.2 K and in perpendicular to the interface magnetic fields up to 330mT. Four-terminal resistance is measured

with a lock-in with current excitation from 2 to 46nA at frequencies between 12 and 32Hz strictly in the linear response. The measurements were performed for a set of gate-voltages fixed during a cool-down. The setup is equipped with a calibrated thermometer in the vicinity of the sample, which allowed to measure the T -dependence of the PC resistance during a slow (more than 1 hour) cool-down or warm-up procedure. Rare random jumps in the resistance on the order of 1%, typically observed above 2K (see figs. 2b and 5a), are presumably owing to a nearby impurity recharging. When recording magnetic field dependencies, we compensated for these by a minor shift ($< 3\%$) of the curves in fig. 3b, such that the zero field data points correspond to fig. 2b. Magnetic field sweeps exhibited a small hysteresis (less than $\pm 10\text{mT}$), which was accounted for with the help of Hall voltage measurements. All together we measured three PCs on two samples prepared out of two similar wafers. The results are sample independent and reproducible in respect to thermal recycling, so that only the data for one PC obtained within the same thermal cycle are given below. Throughout the paper we present the data for the PC resistance, which was actually measured in experiment. When comparing to theory, we make use a relation between small contributions to the resistance and the conductance: $\delta R/R_0 = -\delta G/G_0$, with $R_0 = 1/G_0$.

III. PC RESISTANCE IN ZERO MAGNETIC FIELD

Fig.1 shows gate voltage dependencies of the PC resistance (R) for a set of T values. The traces start at $V_g = -0.2\text{V}$, where (and at more positive V_g) the device resistance $\approx 30\Omega$ is dominated by that of a 2DES connected in series. At more negative gate voltage, the 2DES below the left gate depletes. Since the gate metallization consists out of three parts of different widths (inset of fig. 1), this occurs in a gate-voltage range $-0.22\text{V} \gtrsim V_g \gtrsim -0.35\text{V}$. Below $V_g \approx -0.35\text{V}$ all the current flows through the PC constriction formed in the 2DES. The physical width of the PC, as well as the electron density inside it, is tuned by stray electric fields, such that its resistance increases towards more negative V_g . Within the range $-0.5\text{V} < V_g \lesssim -0.35\text{V}$ the gate-voltage dependencies are featureless and the device behaves as a classical PC with the resistance $0.12h/e^2 > R > 0.05h/e^2$ (corresponding to $3.1k\Omega > R > 1.3k\Omega$). At more negative gate voltages $V_g < -0.5\text{V}$ a smooth transition to a quantum PC regime is observed. Signatures of the quantized resistance plateaus $h/(2ne^2)$ ($n = 1, 2, 3, 4$) are seen at $T \approx 0.47\text{K}$, and washed out completely at higher T . Smearing of the resistance plateaus in fig. 1 is caused by a thermal broadening of the Fermi distribution function⁵. At much lower temperatures, clearly quantized plateaus are routinely observed in our devices¹⁶. In what follows, we focus on a pronounced negative T -dependence of the

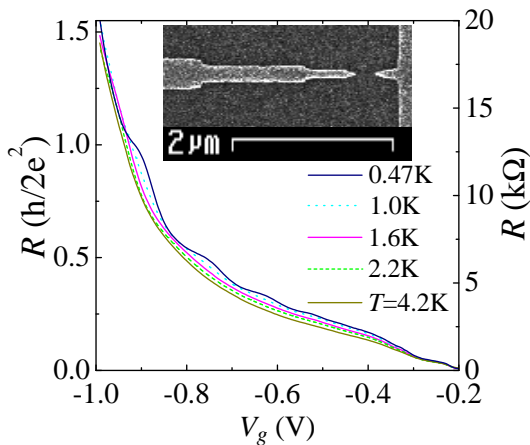


FIG. 1. Gate-voltage dependencies of a four-terminal PC resistance for a set of temperatures in absolute (right axis) and dimensionless (left axis) units. Inset: electron micrograph of the surface of a sample analogous to that used in experiment. Two top gates arranged in a T-shaped geometry appear in a light-grey color.

resistance, which is similar to the results of Ref.¹² and observed within the whole gate-voltage interval in fig. 1.

In fig. 2a the T -dependence of the PC resistance is shown for $V_g = -0.337\text{V}$ (symbols). The data are plotted in the form of T -dependent contribution $-\delta R \equiv -(R(T) - R_0)$, where $R(T)$ is the measured resistance at a given temperature and R_0 is the resistance in the limit $T \rightarrow 0$. For the reasons discussed later (section VI), a direct extrapolation of the T -dependence towards $T = 0$ is not obvious. More accurate is the value of R_0 determined from the magnetoresistance data, see section IV. The overall T -dependence of the PC resistance in fig. 2a is negative, such that $-\delta R$ monotonously increases with increasing temperature. The T -dependence is strongest for $1\text{K} \lesssim T \lesssim 2\text{K}$, where $-\delta R$ increases by a factor of 2.3 almost linearly with T . At higher temperatures, the T -dependence becomes substantially weaker and $\delta R(T)$ tends to saturate. Since $\delta R(T = 0) = 0$, the data imply that the T -dependence should also weaken at $T \rightarrow 0$. This tendency is indeed seen for $0.5\text{K} < T < 1\text{K}$, although not yet pronounced.

Similar qualitative behavior is observed in a wide range of gate-voltages, as shown in fig. 2b. Here the relative contribution $-\delta R/R_0$ is plotted as a function of T for a set of PC resistances $0.64\text{k}\Omega \leq R_0 \leq 6.4\text{k}\Omega$. Again, the negative T -dependence is strongest at intermediate T , and weakens at high and low T , with some minor differences. For instance, the lowest resistance trace ($R_0 = 0.64\text{k}\Omega$) demonstrates a high- T downturn, which seems to have the same origin as the saturation of the T -dependencies for higher R_0 (see section VIA). At $T < 1\text{K}$ three traces on the high R_0 end suffer from a residual thermal smearing of the $n = 2, 3, 4$ resistance

plateaus. This effect contributes a spurious positive (negative) T -dependence on a low- V_g (high- V_g) edge of the resistance plateau⁵. As a result, below 1K the measured T -dependence is stronger for the $6.4\text{k}\Omega$ trace and weaker for the $4.7\text{k}\Omega$ and $3.5\text{k}\Omega$ traces, see the inset of fig. 2b.

The data of fig. 2 demonstrate a negative T -dependence of the PC resistance on the order of $\sim 10\%$ at liquid He temperatures. This effect is observed in a wide range of resistances from the limit of classical PC ($R_0 \ll h/e^2$) to the quantum PC regime (up to $R_0 \approx h/4e^2$). The negative T -dependence of the resistance cannot be interpreted in terms of a backscattering of the electrons owing to a finite elastic mean-free path in the 2DES. In our ballistic PC, the overall backscattering contribution is too small (on the order of $a/l_0 \sim 1\%$) and would result in a positive T -dependence of the resistance. One can also safely neglect a possible contribution from the weak-localization in the 2D leads, which results in a negative T -dependent contribution several orders of magnitude smaller than that in fig. 2. Instead of single-particle effects, we attribute the T -dependence of the PC resistance to the e - e scattering scenario¹³, which turns out to be very well consistent with the experiment (see section VI). Behavior of the magnetoresistance data in small perpendicular magnetic fields, presented in the next section, further supports this conjecture.

IV. PC RESISTANCE IN A PERPENDICULAR MAGNETIC FIELD

The e - e scattering contribution to the PC resistance is predicted to be suppressed by a perpendicular magnetic field $B \neq 0$, as a result of time-reversal symmetry breaking¹⁴. This effect comes from the fact that the trajectories of the two scattering electrons are bent by the magnetic field in a different way, such that the interaction time and the scattering probability decrease compared to the $B = 0$ case. Corresponding magnetoresistance contribution should be positive, T -dependent and observable already in tiny magnetic fields, where the cyclotron radius in the 2DES $R_C = \hbar k_{FC}/eB$ is much larger than the size of the orifice¹⁴.

In fig. 3b the experimental PC magnetoresistance is plotted for a set of temperatures and a gate-voltage $V_g = -0.41\text{V}$. In small fields, the curves $R(B)$ demonstrate a negative T -dependence. The dependence is strongest at $B = 0$ and quickly suppressed in magnetic field. As a result, a pronounced zero-field resistance minimum is observed, which becomes wider and deeper as the T is raised. The T -dependent magnetoresistance is well seen even for $|B| < 10\text{mT}$, where the cyclotron radius ($R_C > 4\mu\text{m}$) by far exceeds the size of the PC orifice. This observation gives a strong evidence for the importance of the e - e scattering for the T -dependence of the PC resistance. In higher magnetic fields $|B| \gtrsim 50\text{mT}$ a sign change of the T -dependence is observed in fig. 3b (signatures of such a behavior were also seen in¹²), which

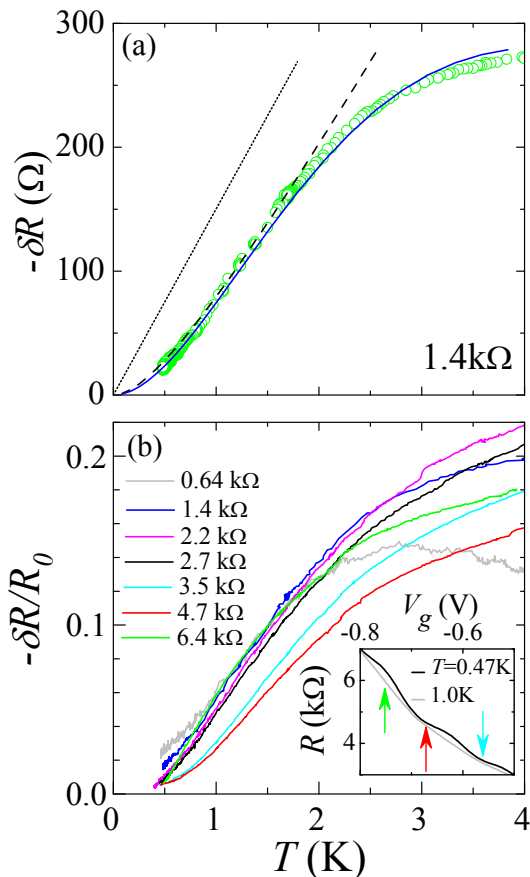


FIG. 2. Temperature dependent contribution to the PC resistance in the absence of magnetic field. (a): experimental T -dependence for $R_0 \approx 1.4 \text{ k}\Omega$ in absolute units (symbols). Model fits are shown by lines, see section VIA. A fit according to eq. (2) for $\alpha_{ee} = 0.77$, $a = 2 \times 290 \text{ nm}$ and $l_c = 13 \mu\text{m}$ is shown by a dotted line. A result of numeric calculation in spirit of Ref.¹³ is shown by a dashed line for the same parameters. This fit is intended to describe deviations from linear T -dependence at low temperatures. A solid line demonstrates a numerical calculation with an account of a beam decay effect owing to e - e scattering. The parameters are $\alpha_{ee} = 1.75$, $l_c = 5 \mu\text{m}$ and the same a . (b): normalized experimental T -dependencies for a set of R_0 indicated in the legend. Inset: gate-voltage dependencies of the PC resistance for the two lowest temperatures. Arrows indicate the points where the three curves on the high R_0 end in (b) were taken.

we failed to unambiguously interpret. For this reason, in the following we limit our analysis of the e - e scattering contribution to the magnetic field range $|B| \leq 25 \text{ mT}$.

Before analyzing the T -dependent contribution in detail, we note, that in fig. 3b it is superimposed on a well-known single-particle magnetoresistance²² (see also¹⁴). The latter contribution is independent of T , and can be identified in the low- T limit. In fig. 3a the PC resistance at the lowest $T \approx 0.47 \text{ K}$ is plotted as a function of B (thick line) for the same V_g as in fig. 3b. Overall magnetoresistance is negative and well explained

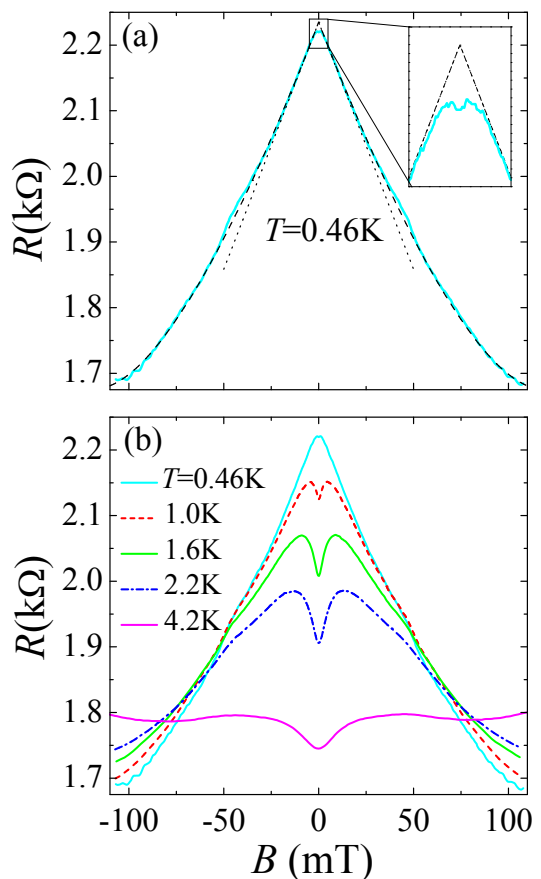


FIG. 3. Magnetoresistance of the PC for $R_0 \approx 2.2 \text{ k}\Omega$. (a): experimental dependence $R(B)$ for the lowest accessible T (solid line) and the fits accounting for the suppression of backscattering in $B \neq 0$ (dotted line) and, additionally, for the magnetoelectric subbands depopulation (dashed line). Inset: magnified low- B region of the main figure with dimensions $45 \Omega \times 10 \text{ mT}$. The experimental data in the inset (solid line) are obtained in a separate low- B sweep with a better resolution. The fits in (a) are obtained assuming the electron densities of $8.3 \cdot 10^{10} \text{ cm}^{-2}$ and $3.15 \cdot 10^{10} \text{ cm}^{-2}$, respectively, in the 2DES and inside the PC. The deduced R_0 equals 2235Ω . (b): evolution of the experimental magnetoresistance with temperature.

by two single-particle effects. The first contribution results from a non-additivity of the ballistic PC resistance and Hall resistance $R_H = B/(ecn_S)$ of the neighboring 2DES leads (so-called suppression of backscattering²¹). In a quasiclassical approximation²², the four-terminal PC resistance exhibits a negative linear magnetoresistance $\delta R(B) = -|R_H| \propto -|B|$. As seen from fig. 3a, for $|B| \leq 25 \text{ mT}$ the experimental magnetoresistance has the same slope as that of $-|R_H|$ (dots) with a value of n_S deduced from Shubnikov oscillations in the bulk 2DES. In stronger magnetic fields, the experimental magnetoresistance weakens, owing to a second effect — depopulation of magnetoelectric subbands in the PC²². To the lowest order in B , this effect contributes a positive magnetore-

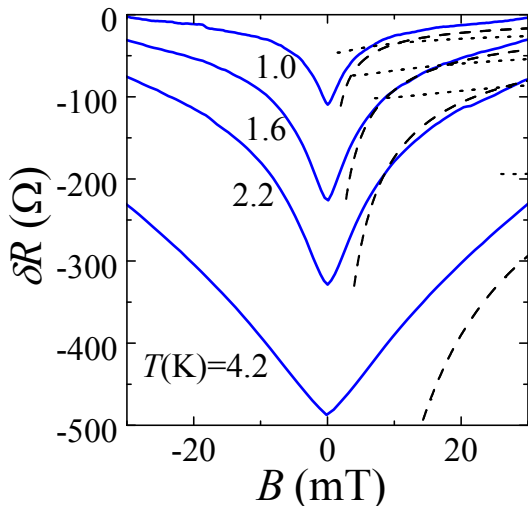


FIG. 4. Magnetic field suppression of the T -dependent correction to the PC-resistance. Experimental data (obtained from fig. 3b, see text) are shown with solid lines. The best fit with eq. (3) (parameters $\alpha_{ee} = 0.3$, $a = 204\text{nm}$, $R_0 = 2235\Omega$ with an assumed density inside the PC $3.15 \cdot 10^{10}\text{cm}^{-2}$) and the empiric fit $\delta R_{ee} \propto T^2 |B|^{-0.7}$ are shown with dotted and dashed line, respectively.

sistance $\propto B^2$. As shown in fig. 3a, taking both these contributions into account results in a nearly perfect fit (dashed line) to the experimental curve for $|B| \leq 100\text{mT}$. Hence, other possible B -dependent contributions (including e - e scattering¹⁴) are negligible at this temperature and the data essentially corresponds to the $T \rightarrow 0$ limit, except for a tiny field range magnified in the inset of fig. 3a.

In the inset of fig. 3a, the experimental magnetoresistance is shown along with the fits of fig. 3a extrapolated towards $|B| \rightarrow 0$. At $B = 0$, the single-particle extrapolation predicts the resistance slightly higher than actually measured, consistent with the negative T -dependence of the zero-field PC resistance of fig. 2. We conclude that at the lowest T used the e - e scattering contribution survives for $|B| < 3\text{mT}$ and causes a residual deviation from the extrapolated single-particle fits. This deviation being small ensures that the complete fit to the lowest T magnetoresistance data (dashed line in fig. 3) can serve as a reliable $T \rightarrow 0$ limit¹⁷. This fit is used as a reference curve $R^{REF}(B)$ to determine the T -dependent contribution $-\delta R(B, T) = R^{REF}(B) - R(B, T)$, where $R(B, T)$ is the measured resistance at a given magnetic field and temperature. The same procedure is performed at every gate-voltage value. Possible systematic error ($< 1\%$) in chosen $R^{REF}(B)$ is not important as long as $|\delta R|/R_0$ is not too small, i.e. for $T \geq 1\text{K}$ and in not too high magnetic fields.

In fig. 4 the B -dependencies of $\delta R(B, T)$, obtained from the data of fig. 3b as described above, are plotted for a set of temperatures. The absolute value $|\delta R|$

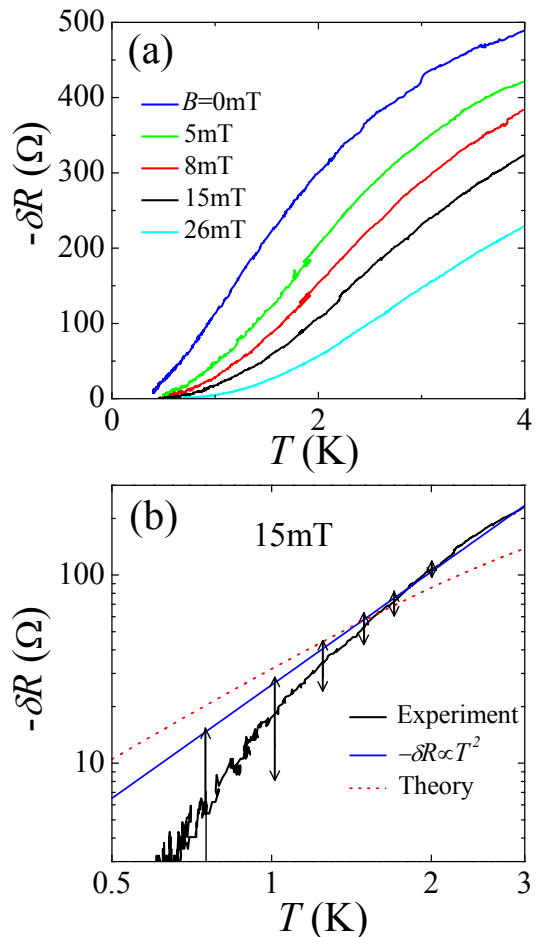


FIG. 5. Evolution of the T -dependence with magnetic field for $R_0 \approx 2.2k\Omega$. (a): experimental T -dependencies plotted in linear scale for a set of magnetic field values. (b): double-log plot of the experimental dependence at $B = 15\text{mT}$, together with the fit to eq. (3) (parameters $\alpha_{ee} = 0.3$, $a = 204\text{nm}$, $R_0 = 2235\Omega$ with an assumed density inside the PC $3.15 \cdot 10^{10}\text{cm}^{-2}$) and the empiric dependence $\delta R \propto -T^2$. The arrows indicate an uncertainty of the zero- T limit of the PC resistance $\pm 10\Omega$.

is maximum at $B = 0$, symmetric with respect to field reversal and decays in magnetic field. The functional B -dependence weakens as the magnetic field is increased. This behavior is qualitatively consistent with the prediction¹⁴ for the e - e scattering contribution. Dashed lines in fig. 4 show the best empiric power law fit to the experimental data set with an expression $\delta R \propto -T^2 B^{-0.7}$. We find such a fit reasonable at intermediate temperatures $T \leq 2.2\text{K}$ except for small $|B|$. Scaling of the magnetoresistance data at different V_g (section V) indicates that similar functional B -dependencies $-\delta R(B)$ are observed in a wide range of the PC gate voltages.

In fig. 5a the measured T -dependencies are plotted for a set of fixed (positive) B values. At $B = 0$, as discussed above, a nearly linear T -dependence is observed for $T < 2\text{K}$, followed by saturation at higher T . The

B -driven suppression of the T -dependent contribution is stronger at lower T . As a result, with increasing B the T -dependence becomes closer to parabolic at low temperatures. This behavior is in line with the predictions for the e - e scattering¹⁴.

For a quantitative analysis of the T -dependence we plot the data at $B = 15$ mT on a double logarithmic scale in fig. 5b (thick solid line). The experimental uncertainty is indicated by arrows with the following meaning. The reference value $R^{REF}(B)$ is determined with an accuracy of $\pm 10\Omega$, appreciably worse than the random error in measured T -dependence ($\pm 2\Omega$). This unknown additive contribution to $\delta R(T)$ could shift the data up or down as a whole, to a position somewhere between those indicated with arrows in fig. 5b. Within this uncertainty, the experimental data is compatible with a power-law $\delta R(T) \propto -T^\alpha$, where $\alpha \approx 2.5 \pm 0.5$. An example of parabolic fit $-\delta R \propto T^2$ is shown by a thin solid line in fig. 5b.

V. SCALING THE MAGNETORESISTANCE DATA AT DIFFERENT GATE-VOLTAGES

In fig. 6a we compare the curves $\delta R(B)$ taken at $T = 1.6$ K for two different V_g corresponding to the PC resistances of $R_0 \approx 1.4k\Omega$ and $R_0 \approx 3.4k\Omega$. In both cases, the overall effect of magnetic field is qualitatively similar to that in fig. 4 and the absolute value $|\delta R(B)|$ increases with R_0 . At the same time, the width of the V-shaped dependence along the B -axis also increases with R_0 , as demonstrated by arrows in fig. 6a, which mark the full width at the half minimum $\delta R(B)$. This behavior is observed within the whole range of R_0 investigated and for all T used.

We find that the data $\delta R(B)$ at different R_0 permit a single parameter scaling. At a given T , an empiric relation $a_{eff}^{-1}\delta R/R_0 = F(a_{eff}B)$ approximately holds, where a_{eff} is an R_0 -dependent scaling parameter and F is a function which determines the shape of the B -dependence at this T . It is convenient to express a_{eff} in units of length and plot the scaled B -dependencies in dimensionless coordinates $\delta R/R_0 \cdot w/a_{eff}$ vs $\beta \equiv a_{eff}/R_C$, where $w = 130$ nm is a lithographical half-width of the PC and $R_C \propto B^{-1}$ is a cyclotron radius in the 2DES. This choice of axes is natural for the e - e scattering mechanism of the T -dependence, as explained in section VI.

In fig. 6b, we plot the results of the scaling procedure for a wide range of R_0 . For each of the four temperatures used, the data are obtained as follows. We vary the value of a_{eff} such that the dependencies $\delta R(B)/R_0$ at different R_0 fall on a single curve. For better scaling, the value of R_0 is also slightly varied within the corresponding experimental uncertainty (see fig. 2 of the supplementary material). At a given T , a nearly perfect scaling is obtained in the region of not too high $|\beta|$, where $\delta R(B)/R_0$ is not small, and outside the very vicinity of $\beta = 0$ (zero magnetic field). The scaling is successful even far from

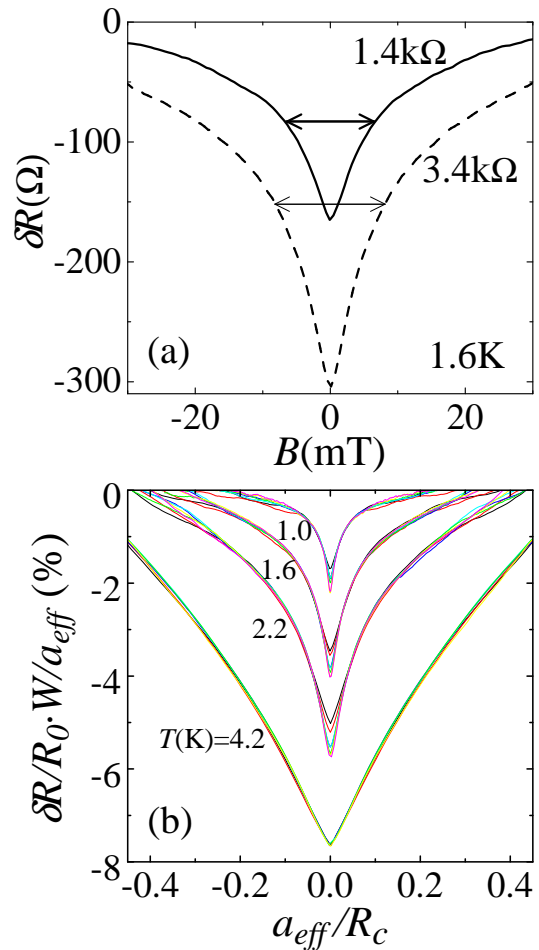


FIG. 6. Magnetoresistance at different R_0 . (a): experimental dependencies $\delta R(B)$ for two values of R_0 at 1.6 K. Arrows mark full width at the half minimum of the V-shaped dependencies. (b): One-parameter scaling of the magnetoresistance data for $R_0 \leq 6.4k\Omega$. The temperature increases from top to bottom $T = 1, 1.6, 2.2, 4.2$ K.

the classical PC limit, up to $R_0 \approx h/4e^2$. Remarkably, a similar low- B behavior is observed even close to the resistance quantum h/e^2 , although the scaling is worse for such high R_0 (not shown).

In fig. 7 we plot the scaling parameter a_{eff} (symbols) as a function of R_0 . The absolute value of a_{eff} is not determined in a scaling procedure and is chosen to coincide with the physical half-width a of the PC on the lowest R_0 end. Normalized in this way, a_{eff} is nearly T -independent and decreases at increasing R_0 . As seen from fig. 7, a_{eff} drops by less than a factor of 3 when R_0 is varied by almost an order of magnitude.

VI. DISCUSSION

As demonstrated in previous sections, the resistance of a ballistic PC in a high-quality 2DES exhibits a negative

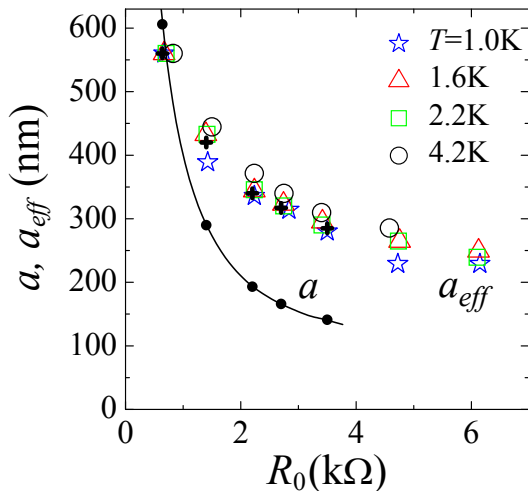


FIG. 7. Dependence of the scaling parameter a_{eff} from fig. 6 (symbols) and physical half-width a of the PC (line) on R_0 . The physical half-width a is evaluated from eq. (1) with $G_0 = 1/R_0$, with a reduced electron density inside the PC taken into account (see Appendix A). The scaling parameter a_{eff} , normalized as described in the text, is shown by separate symbols for the four temperatures used. Black dots and crosses mark, respectively, the values of a and a_{eff} used in numerical fits, see Appendix B.

T -dependence at liquid He temperatures. In the absence of magnetic field, the T -dependence is relatively strong below $T \approx 2\text{K}$ and tends to saturate at higher temperatures. At not too high T , a small magnetic field on the order of a few 10mT tends to suppress the T -dependence. These observations can only be explained in terms of the e - e scattering contribution to the ballistic PC resistance. The experimental data is qualitatively consistent with the predictions of Refs.^{13,14} for classical PCs. Below we discuss the experimental results in detail, quantitatively compare the experimental behavior with key theoretical predictions and attempt to evaluate the strength of the e - e scattering in the 2DES studied.

A. Zero magnetic field

a. Qualitative picture at not too high T . At temperatures in the range $0.5\text{K} < T \lesssim 2\text{K}$, the experimental T -dependence of the resistance is not far from linear (see symbols fig. 2a). Still, at low T the dependence is incompatible with the proportionality $|\delta G_{ee}| \propto T$ predicted by eq. (2). This is strongly supported by the magnetoresistance data of section IV, where the contribution of e - e scattering is almost negligible at the lowest temperature used $T \approx 0.5\text{K}$. This behavior is captured by a numerical calculation of the e - e scattering contribution in spirit of Ref.¹³ (see Appendix B for the details) and can be qualitatively understood as follows.

Consider a scattering of an injected electron (momen-

tum \mathbf{k}) with the one incident onto the PC (momentum \mathbf{p}) at large distances r from the orifice ($r \gg a$). The two momenta are approximately opposite, such that the angle φ between \mathbf{k} and $-\mathbf{p}$ is small: $|\varphi| \leq \phi_{PC} \ll 1$, where $\phi_{PC} = a/r$ is the angular dimension of the PC orifice at a distance r . For $|\varphi| \leq \phi_T$ (with a thermal angle defined as $\phi_T \approx T/E_F$), the two electrons can scatter by an arbitrary angle⁹ and the scattering probability is independent of φ . Outside this range, for $|\varphi| > \phi_T$, the scattering probability decreases with increasing $|\varphi|$ and, accordingly, the scattering angle cannot exceed $\sim \phi_T/|\varphi|$. These constraints result from the conservation laws and the Pauli principle. Depending on T and/or r , two limiting cases can be realized.

Fig. 8 sketches the momentum space for the two limiting cases. A situation of fig. 8a is realized when $\phi_{PC} < \phi_T$, i.e. at not too low T (and/or not too small r). In this case, an average injected electron (shown by a black dot) can scatter by an arbitrary angle with each of the electrons within the stripe $|\varphi| < \phi_T$ of the width $\sim T$ (shown by a light grey color). However, only the scattering with the electrons within the angle $|\varphi| \lesssim \phi_{PC}$ can contribute to the PC conductance. Hence, $\delta G_{ee} \sim \phi_{PC} \times T$, which in the end gives rise to the linear T -dependence and a log-dependence on l_c in eq. (2), derived in Ref.¹³. At $T \rightarrow 0$ the condition $\phi_{PC} < \phi_T$ breaks down and one expects deviations from the linear T -dependence. In fig. 8b we sketch a situation in the limit of very low T , such that $\phi_T \ll (\phi_{PC})^2$. Here an average injected electron (black dot) cannot effectively scatter an incident electron unless $|\varphi| \lesssim \phi_T/\phi_{PC}$. The corresponding momentum space region of width $\propto T$ is shown by a light grey color in fig. 8b. Outside this region, for larger $|\varphi|$, the typical scattering angle is smaller than ϕ_{PC} . Corresponding scattering processes do not influence the conductance for one of the scattered electrons still reaches the PC orifice. In this limit the e - e scattering contribution acquires a parabolic²⁵ T -dependence $\delta G_{ee} \propto T^2$.

The dashed line in fig. 2a represents a numerical fit to the experimental data (symbols) performed in the framework of Ref.¹³. The calculation exhibits a crossover between the two limiting cases considered above and is quantitatively consistent with the experiment at $T \leq 2\text{K}$ for the chosen fit parameters (see caption). For comparison, the dependence predicted by eq. (2) for the same fit parameters is shown by the dotted line in fig. 2a. Note that the numerically calculated T -dependence is strongly nonlinear below 0.5K. This demonstrates that a naive linear extrapolation of the experimental dependence $R(T)$ towards $T = 0$ may be misleading and an independent determination of R_0 is needed (see section IV). The low- T behavior is related to the value of the cutoff length l_c , which is expected to be comparable to the elastic mean-free path¹³. As discussed in Appendix B, at increasing l_c the numerical result asymptotically approaches the analytic prediction of eq. (2) for arbitrarily low temperatures. Hence, a proportionality¹³ $\delta G_{ee} \propto T$ might be observed in samples of exceptionally high quality in fu-

ture (see Appendix B).

b. High- T behavior and beam decay effects. As seen from fig. 2a, the experimental T -dependence levels off and tends to saturate at $T > 2\text{K}$. Similar behavior $\delta R(T)$ is observed within the whole range of gate-voltages studied (fig. 2b), which is not predicted by theory¹³. We find that such a qualitative behavior is in fact expected for the e - e scattering scenario at high enough T and is related to a breakdown of a condition $l_c \ll l_{ee}$, where l_{ee} is an electron mean-free path for e - e scattering. In such a situation, a decay of the injected beam on the length scale of l_{ee} owing to the e - e scattering is not negligible. Therefore, the total e - e scattering probability is no longer small and the calculations¹³ to first order in α_{ee} are expected to overestimate the effect of e - e scattering on the PC conductance.

One can estimate the length l_{ee} based on a calculation of a quasiparticle lifetime¹⁹. This calculation agrees with energy-relaxation data in a high-density device²⁰. In our 2DES at $T = 4\text{K}$ such an estimate gives $l_{ee} \approx 2.7\mu\text{m}$, indeed, much smaller than the elastic mean-free path l_0 . Moreover, we estimate that the condition $l_0 \sim l_c \ll l_{ee}$ is satisfied only at $T \ll 2\text{K}$. Therefore, the applicability range of the numeric calculation in spirit of Ref.¹³ turns out too narrow for a reliable estimation of the e - e interaction parameter α_{ee} . Unfortunately, a mathematically strict account for the effects of the beam decay owing to e - e scattering is too involved for modeling. Nevertheless, we performed additional numerical calculations with an ad-hoc introduced decay of the injected beam with characteristic length-scale of l_{ee} . These calculations are capable of reproducing the T -dependence in the whole temperature range studied, see Appendix B. One such fit perfectly consistent with the experiment is plotted by a solid line in fig. 2a. Note that the interaction parameter α_{ee} obtained from such fits roughly 2 times larger compared to the fit with the beam decay effect disregarded (dashed line in fig. 2a).

B. Finite magnetic field

Thanks to the time-reversal symmetry breaking, the contribution of the e - e scattering to the PC conductance is expected to rapidly decay in a perpendicular magnetic field¹³. The theoretical prediction of Ref.¹⁴ for not too small magnetic fields is given by:

$$\frac{\delta G_{ee}}{G_0} = \frac{2}{9} \alpha_{ee} \frac{ak_F}{\sqrt{\beta}} \frac{T^2}{E_F^2} \ln \left(\beta \frac{E_F^2}{T^2} \right). \quad (3)$$

This result is derived assuming $T^2/E_F^2 \ll \beta \ll 1$, where $\beta \equiv a/R_C \propto B$ is the ratio of the half-width of the PC orifice to the cyclotron radius in the 2DES $R_C = \hbar k_{FC}/eB$.

Eq. (3) predicts that a decay of δG_{ee} in a perpendicular magnetic field causes a T -dependence stronger than that in $B = 0$. On the other hand, as follows from this

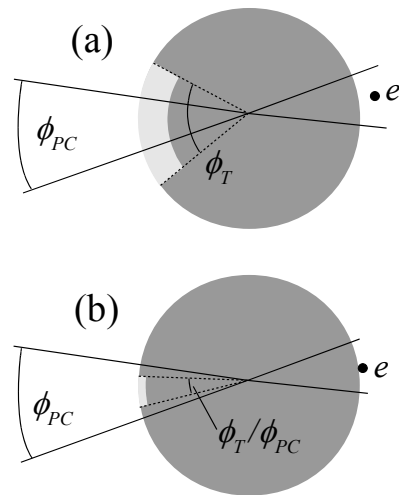


FIG. 8. A sketch of momentum space in the 2DES at a distance $r \gg a$ from the orifice for two limiting cases of not too low T (or large r : $\phi_T \gg \phi_{PC}$) (a) and very low T (or small r : $\phi_T \ll (\phi_{PC})^2$) (b), see text. A typical state of a non-equilibrium electron injected through the PC is shown by a black dot. Dark grey color indicates occupied states below Fermi surface. Electron states with approximately opposite momenta available for e - e scattering are shown as light grey areas (see text for the details).

expression, at higher temperatures a decay of δG_{ee} occurs in stronger magnetic fields scaling as $\sqrt{\beta} \propto T$. This behavior has to do with the physics of e - e scattering in perpendicular magnetic field. Quasiclassically, the e - e scattering probability is proportional to the effective interaction time between the scattering electrons. The interaction time depends on the angle φ between the momenta \mathbf{k} and $-\mathbf{p}$ (see section VIA). In $B = 0$ case, this time is maximum for electrons with opposite momenta ($\varphi = 0$), which follow time-reversed trajectories. As derived in Ref.¹⁴, in finite B the time-reversal symmetry is broken and the maximum interaction time is attained for scattering of electrons with a nonzero angle: $|\varphi| \propto \sqrt{\beta}$. Along with the phase space argument of section VIA this explains the $B - T$ scaling mentioned. The low- B experimental data of figs. 4 and 5a are in perfect qualitative agreement with these theory predictions, strongly supporting our interpretation in terms of the e - e scattering scenario of Refs.^{13,14}.

The functional T - and B -dependencies predicted by expression (3) are weaker than observed in experiment. Dotted lines in fig. 4 represent an effort to fit the experimental B -dependence with expression (3) in the range of magnetic fields where it's applicable. Despite the overall trends are qualitatively captured by the fits, we observe that a functional B -dependence in the experiment is appreciably stronger than the theory predicts. Except for the highest $T = 4.2\text{K}$, the empiric dependence of the form $\delta R \propto T^2 B^{-0.7}$ describes the data much better in the same range of B (dashed lines in fig. 4).

The T -dependence in magnetic field is also somewhat stronger than the theoretical prediction. The dashed line in fig. 5b, drawn according to eq. (3), is not consistent with the experimental dependence (thick solid line) in a typical magnetic field of $B = 15\text{mT}$. At the same time, the empiric parabolic dependence $|\delta R(T)| \propto T^2$ can well describe the data within the experimental uncertainty. Note, that the T -dependence of fig. 5b is discussed in a limited range $T \leq 3K$, which is related to a possible problem with the applicability of the theoretical analysis at high temperatures (see section VI A).

Several possibilities might be responsible for the discrepancy between the theory and experiment in magnetic field. First, we mention the unknown positive T -dependence of the resistance seen for $|B| \gtrsim 50\text{mT}$ (fig. 3). If additive with the e - e scattering induced magnetoresistance at lower $|B|$, such a "wrong-sign" contribution can strengthen the dependence $\delta R(B)$. Second, the T-shaped split-gate layout of our sample (inset to fig. 1) is different from the theoretical geometry¹⁴, which might be important for calculation of the effective interaction times performed in theory. Finally, long-range density gradients around the lateral PC and beam collimation effects discussed in the next can well affect the e - e scattering contribution in $|B| \neq 0$.

C. Scaling and a_{eff}

As demonstrated in section V, the experimental dependencies $\delta R(B)$ at different R_0 obey scaling in the form $a_{eff}^{-1} \delta R(B)/R_0 = F(a_{eff}/R_C)$, where the function F determines the shape of the B -dependence at a given temperature. Here we argue that such a scaling is inherent for the e - e scattering problem in a 2DES in magnetic field.

Consider two classical PCs of widths a_1 and a_2 in magnetic fields corresponding to cyclotron radii of, respectively, R_1 and R_2 . Since the phase space for e - e scattering is determined essentially by the angle between the momenta of scattering electrons, these two problems are similar and can be reduced to each other via scaling a spatial coordinate, provided $a_1/R_1 = a_2/R_2$. The only difference is that the total scattering probability (proportional to the interaction time) scales as a_i . Hence, we conclude that the e - e scattering contribution obeys scaling in the form $a^{-1} \delta G^{ee}/G_0 = F(a/R_C)$. It appears that both analytical expressions of Ref.¹⁴ derived in the limits of low and high β obey such a scaling. This universality is expected to breakdown only at very low magnetic fields ($R_C \gg l_c$), where a weak disorder scattering comes into play¹⁴.

As shown in fig. 6b, the experimental dependencies $\delta R(B)$ permit scaling of this kind in a wide range of R_0 and all T used. This further supports our interpretation of the negative T -dependence in small B in terms of the e - e scattering mechanism¹⁴. The scaling also indicates that a problem with a functional dependence $\delta R(B)$, which is

appreciably stronger in experiment than in theory, persists regardless R_0 .

As follows from the above argument, the scaling parameter is proportional to the PC half-width a . Unexpectedly, the evolution of a_{eff} with R_0 in fig. 7 is appreciably weaker than that of the physical half-width a (symbols and line, respectively). This discrepancy could not be ascribed to experimental uncertainties in scaling procedure and/or evaluation of a (see Appendix A). The data of fig. 6b and fig. 7 suggest that a different length-scale $\propto a_{eff}$, rather than a , controls the behavior of the e - e contribution to the resistance of a laterally defined PC in magnetic field. This behavior might be related to a long-range potential landscape nearby the PC, as briefly discussed below.

As a result of stray electric fields from the split-gates, an electrostatically defined PC takes the shape of a finite length channel with smooth boundaries. This causes a classical beam collimation effect in lateral PCs²⁶. A reduced electron density inside the PC also results in beam collimation via an electrostatic lens effect^{22,27,28}. In a model of a horn-shaped channel²², the angular dimension of the collimated (injected or incident) electron beam is reduced compared to π . This is compensated by the increased channel width a_{exit} at the exit (entrance) of the PC, although the conductance G_0 is still given by the minimum channel width a and eq. (1). Hence, the angular dimension of the PC observed at large distances is increased: $\phi_{PC} \propto a_{exit} > a$, which is expected to enhance the relative e - e scattering contribution. This effect resembles the operation of a microwave horn antenna. In addition, the collimated beam is squeezed towards the normal to orifice, so that the angular dimension of the orifice is, on the average, further increased: $\phi_{PC} \propto \cos \phi_n$, where ϕ_n is the angle in respect to the normal to orifice. Obviously, both effects become more pronounced as the PC is being depleted. One can speculate, that at large l_c these effects might be roughly described by an extra effective width parameter $a_{eff} > a$ used instead of a in eq. (2). Independent experiments could verify whether the results of our scaling procedure in magnetic field can be interpreted in this way.

D. Evaluation of the interaction parameter α_{ee}

The Coulomb interaction in a 2DES is modified owing to screening and correlation effects²³. E - e scattering provides an important information about interactions via a scattering length (cross-section in 2D) $\lambda(\theta)$, where θ is a scattering angle²⁴. The total scattering probability can be expressed through a total scattering length $\lambda_{tot} = \int_0^\pi \lambda(\theta) d\theta$. In a classical approach of Refs.¹³⁻¹⁵ this is determined by a dimensionless interaction parameter α_{ee} : $\lambda_{tot} = \pi \alpha_{ee}/(4k_F)$. The measurement of the e - e scattering contribution to the PC resistance gives a direct access to the scattering length in the 2DES.

Eq. (2) permits determination of α_{ee} from the slope

of the T -dependence at $B = 0$, provided the constriction half-width a and the cutoff length l_c are known. Moreover, analysis of the B -dependence of the e - e correction allows to exclude an uncertainty related to the unknown cutoff length l_c , as follows from eq. (3). However, application of this procedure to the present experiment is problematic owing to the discrepancies between theory and experiment discussed above. Still, we attempt to evaluate α_{ee} fitting the zero field data $\delta R(T)$ by a numerical calculation in spirit of Ref.¹³.

As discussed above, at temperatures used in our experiment the estimated mean-free path for e - e scattering is typically not large compared to the elastic mean-free path (and l_c), so that the electron beam decay should be taken into account. We employ fits with a numerical calculation, which accounts for the beam decay on the length-scale of the mean free path for the e - e scattering. Such fits are capable to describe the data within the whole T -range (see Appendix B) and serve as an order of magnitude estimate for α_{ee} .

At a given R_0 , the dependence $\delta R(T)/R_0$ from fig. 2b is numerically fitted with three fit parameters a , l_c and α_{ee} . The best fits are obtained for $l_c = 5\mu\text{m}$ (for $R_0 > 0.64k\Omega$). We used a separate value of $l_c = 8.5\mu\text{m}$ when fitting the lowest PC-resistance data ($R_0 = 0.64k\Omega$), which best reproduces a downturn on the T -dependence (see fig. 12). These values of the cutoff length are substantially smaller than the elastic mean-free path in our device ($l_0 \approx 20\mu\text{m}$). This discrepancy might arise from a crude model used and is not crucial for our purposes. Important for the evaluation of α_{ee} is the knowledge of the parameter a . For a classical PC a simply equals the half-width of the orifice^{13,14}. However, this is not the case in present experiment for the following reason. In our T-shaped split-gates layout about a half of the electrons can reach the PC after a scattering off the 2DES boundary defined by the right-hand-side gate in the inset of fig. 1. Assuming a specular boundary scattering, this results in a factor of 2 enhanced a compared to the geometry of Ref.¹³ at the same R_0 . Therefore we perform a numerical fit with a equal twice the physical half-width of the PC. We also perform an extra fit using effective width $a = 2a_{eff}$, as suggested by the scaling of the experimental curves $\delta R(B)$ in magnetic field.

The interaction constant obtained from such numerical fits is plotted in fig. 9 as a function of R_0 in the range $0.6k\Omega < R_0 < 3.5k\Omega$ (symbols). Circles and triangles correspond to fitting with a determined by the physical width and the effective width, respectively. Error bars in the figure indicate an estimated random uncertainty of the evaluation procedure, which is mainly limited by that of the R_0 determination. For each data set α_{ee} is roughly independent of R_0 (exception is the case of $R_0 = 0.64k\Omega$), as expected for the parameter characterizing the strength of the e - e scattering in the 2DES. Based on fig. 9 we conclude that our experiment is consistent with an order of magnitude estimate¹³ $\alpha_{ee} \sim 1$. A direct calculation²⁴ of the 2D scattering length predicts

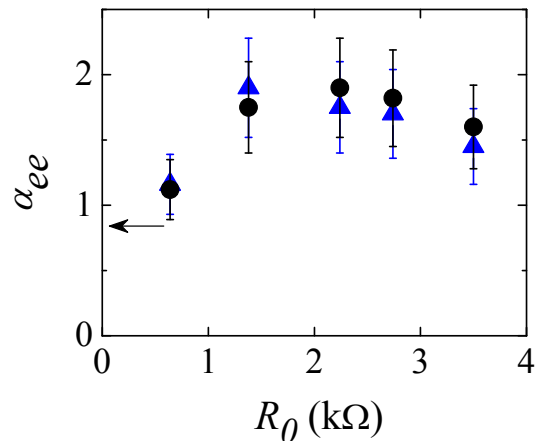


FIG. 9. Evaluation of α_{ee} from the zero field T -dependence. Circles and triangles correspond to fitting with a determined by the physical width and the effective width, respectively, as explained in the text. The values of a and a_{eff} used for fitting are shown in fig. 7 as dots and crosses, respectively. Error bars ($\pm 20\%$) mark the random uncertainty of the evaluation procedure. The arrow points at the value expected from the calculation²⁴ of e - e scattering length (see text).

comparable values of the interaction parameter, which increases at decreasing the 2D electron density. We were able to check that at a density of $n_S = 1.5 \times 10^{11} \text{cm}^{-2}$, still almost twice higher than that in our 2DES, the calculations²⁴ predict $\alpha_{ee} \approx 0.84$ (at $T = 2\text{K}$). This value, shown by an arrow in fig. 9, is roughly consistent with our evaluation. Unfortunately, a systematic uncertainty, associated with our fitting procedure and large number of fit parameters, by far exceeds the random uncertainty in fig. 9. This doesn't permit a quantitative comparison beyond the order of magnitude estimate. The data of fig. 9 is rather meant to illustrate that in a wide range of R_0 the absolute value $\delta R(T)$ is roughly consistent with the predictions of the e - e scattering scenario.

VII. SUMMARY

In summary, we studied a T -dependent contribution δR to the resistance of a ballistic PC in a 2DES of a high-quality GaAs/AlGaAs heterostructure at temperatures below 4.2K. In zero magnetic field, the resistance decreases by ~ 10 – 20% as the temperature is raised from 0.5K to 4.2K. The dependence is roughly linear below 2K and weakens at higher T . A B -driven suppression of δR is found in perpendicular magnetic fields of a few 10mT and not too high T . These results give strong evidence for the influence of the e - e scattering on the PC conductance. The observations are similar in a wide range of R_0 , even outside the classical PC regime, and can be qualitatively described with the e - e scattering scenario of Refs.^{13,14}. We argue that in $B = 0$ case the discrepancies between the experiment and theory can be well understood, and

support by a numerical calculation. In magnetic field, the curves $\delta R(B)$ permit single-parameter scaling in a wide range of PC resistances R_0 , which is an intrinsic property of the e - e scattering problem. Contrary to expectations, the dependence of the scaling parameter on R_0 is sufficiently weaker than that of the physical half-width of the orifice. This indicates that the value of the e - e scattering contribution in a lateral PC is determined by an independent parameter a_{eff} , which we call an effective half-width of the PC. In $B = 0$ case, we perform a numerical calculation, which goes beyond theoretical assumptions¹³ and is capable to quantitatively describe the experimental data in whole temperature range. Using this calculation, the interaction constant α_{ee} of the 2DES is evaluated, which is in rough quantitative agreement with the calculations²⁴ of the e - e scattering length in 2DESs in GaAs.

VIII. ACKNOWLEDGEMENTS

We acknowledge discussions with I.L. Aleiner, I.S. Burmistrov, E.V. Deviatov, V.T. Dolgoplov, V.F. Gantmakher, A.A. Shashkin, D.V. Shovkun. We also wish to thank T.V. Krishtop and K.E. Nagaev for discussions and criticism. Financial support from RAS, RFBR, the grant MK-3102.2011.2, the German Excellence Initiative via the Nanosystems Initiative Munich (NIM) and LMUexcellent is gratefully acknowledged. VP and LS wish to acknowledge financial support from Italian Ministry of Research through FIRBIDEAS Project No. RBID08B3FM.

Appendix A: Evaluation of the electron density inside the PC

The resistance R_0 of a quasiclassical PC and its physical half-width a (at a Fermi level) are directly related as $R_0 \propto C_1/(ak_F^{PC})$, where the Fermi wave-vector is given by $k_F^{PC} = (2\pi n^{PC})^{1/2}$ and n^{PC} is the (2D) electron density inside the PC. The numerical coefficient depends on the model of confinement potential and equals $C_1 = \pi$ (4), respectively, for a hard-wall (parabolic) confinement. Separate determination of a and n^{PC} is possible by analyzing the depopulation of the magneto-electric subbands in perpendicular magnetic field.

The depopulation effect gives rise to a positive contribution to the magnetoresistance of the quasiclassical PC, which to the lowest order in B is given by²²:

$$\frac{\delta R_{depop}}{R_0} = C_2 \left(\frac{a}{R_C^{PC}} \right)^2 \propto (C_1)^2 C_2 \frac{B^2}{(n^{PC})^2}, \quad (\text{A1})$$

where $R_C^{PC} = k_F^{PC} \hbar c (eB)^{-1}$ is the cyclotron radius corresponding to the electron density inside the PC. The confinement model dependent coefficient equals $C_2 = 1/6$ (1/2), respectively, for a hard-wall (parabolic) confinement. Here we also used $a \propto C_1/k_F^{PC}$, since R_0 is fixed.

The evaluated density depends on the details of the PC confinement via a factor $C_1(C_2)^{1/2}$ equal to ≈ 1.28 (2.83) for a hard-wall (parabolic) model confinement potential. In fact, a gradual transition from a hard-wall-like confinement in a wider constriction to a parabolic-like confinement in a narrower constriction is typically found²⁹ in agreement with numerical simulations (see²² for references). Here, we evaluate the electron density n^{PC} assuming a hard-wall confinement. In this way a lower boundary for n^{PC} is obtained and the strongest possible gate-voltage dependence of the electron density inside the PC.

The result is shown in fig. 10 for gate voltages in the range corresponding to $0.64k\Omega \leq R_0 \leq 3.5k\Omega$ (symbols). Here, the lowest T experimental data were used, where the contribution of the e - e scattering to the magnetoresistance is not important (see section IV). The evaluated density n^{PC} is reduced by at least a factor of 2 compared to that in the bulk 2DES and further decreases towards the lower V_g . Note that assuming a parabolic confinement would result in factor of 2.2 higher density, that is pretty close to the bulk 2DES value ($n_S \approx 0.83 \cdot 10^{11} \text{cm}^{-2}$). Most probably, the actual density is somewhere in between the two limiting cases.

Strictly speaking, the data scatter in fig. 10 precludes an accurate evaluation of the gate-voltage dependence of n^{PC} . As a crude estimate, we take the simplest capacitive approximation $\delta n^{PC} \propto \delta V_g$ to describe the data, which is reasonable for a relatively deep 2DES used. The dashed line is the best linear fit extrapolating to $n^{PC} = 0$ near the pinch-off point of the PC at $V_g \approx -1.1\text{V}$. It is this fit, that was used for the evaluation of the physical half-width a in fig. 7. Note that a $\approx 16\%$ uncertainty in a associated with the confinement model choice ($a \propto C_1^{1/2} C_2^{-1/4}$) is not crucial for us (see fig. 9). At the same time, an account of a gradual change from a hard-wall-like to a parabolic-like confinement at decreasing V_g could only cause a functional dependence of $a(R_0)$ in fig. 7 to become farther from $a_{eff}(R_0)$.

Appendix B: Numerical calculation

We perform a numerical calculation of the e - e scattering contribution in a 2DES for $B = 0$ in spirit of Ref.¹³. This task involves a 6-dimensional integration:

$$\frac{\delta G}{G_0} = \frac{\alpha_{ee} k_F a}{8\pi^2} \int_0^{\pi/2} \cos \phi_p d\phi_p \int_1^{l_c/a} dr \quad (\text{B1})$$

$$\int d\phi_k \int d\theta \int \int \frac{f_{p'} f_{k'} + f_p - f_p f_{p'} - f_p f_{k'}}{T \cosh^2 \frac{\varepsilon_k - 1}{T}} d\varepsilon_p d\varepsilon_k$$

Here $p, \varepsilon_p(k, \varepsilon_k)$ is the momentum and energy (in units of E_F) of the electron incident to (injected through) the PC orifice, respectively. After scattering the electrons

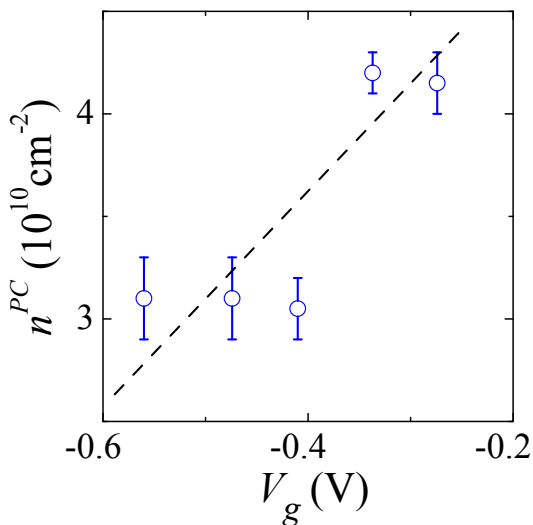


FIG. 10. Evaluation of the electron density inside the PC from subband depopulation effect, assuming a hard-wall confinement. Experimental points for a set of gate-voltages are shown by symbols. These symbols indicate values of the density averaged over several experiments at the same V_g . Error bars represent a random uncertainty, which comes from both the accuracy of the fits and reproducibility of the magnetoresistance traces $R(B)$. The dashed line is the best linear fit $\delta n^{PC} \propto \delta V_g$.

acquire the momenta p' and k' . The angle of p in respect to the direction normal to the orifice is denoted as ϕ_p ; ϕ_k is the angle between the direction towards the center of the orifice and momentum k ; θ is the scattering angle in the relative momentum space. The distance r from the PC is measured in units of PC half-width a (region $r < a$ is omitted) and the temperature T – in units of E_F . The equilibrium distribution functions for the momenta p, p', k' are denoted by $f_p, f_{p'}, f_{k'}$. In this expression we accounted for the energy and momentum conservation laws and substituted the distribution f_k by its nonequilibrium part linearized in respect to bias voltage across the PC. Integration over ϕ_k is restricted to the angular dimension of the electron beam injected through the PC $\phi_k \in (-\phi_{max}, \phi_{max})$, where $\phi_{max} = \arctan(\cos \phi_p / r)$. Integration over θ is limited to the scattering angles such that electrons k' and p' don't reach the orifice. At a given T we restrict the integration over electrons' energies to the interval $E_F \pm 5T$.

In fig. 11 we plot the results of the numerical calculation for $\alpha_{ee} = 1$, $a = 400\text{nm}$ and a set of l_c values between $5\mu\text{m}$ and $100\mu\text{m}$. We find that at high T the slope of the T -dependence is approximately proportional to $\ln(l_c/a)$, in agreement with the analytic result of eq. (2). To illustrate this, for each l_c the calculated relative contribution $\delta G/G_0$ was divided by $\ln(l_c/a)$ in fig. 11 to give approximately the same slope at high T . In the limiting case $l_c \rightarrow \infty$ we recover the result of eq. (2), although the numerical coefficient obtained is a factor of ≈ 1.7 larger.

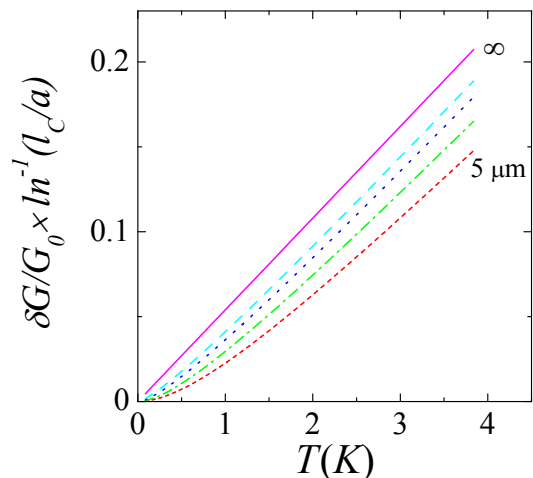


FIG. 11. Results of numerical calculation of the e - e scattering contribution in zero magnetic field. The data correspond to $\alpha_{ee} = 1$, $a = 400\text{nm}$ and a set of $l_c = \infty, 100, 30, 10, 5\mu\text{m}$ from top to bottom curve. The ordinate axis is chosen to illustrate the dependence on l_c , see text.

The origin of this discrepancy is unclear and we compensate for this when fitting the experimental data.

At increasing T a mean-free path l_{ee} for the e - e scattering decreases and eventually becomes comparable to or smaller than the cut-off length scale $l_c \sim l_0$. This means that an electron beam injected through the PC decays at a typical distance of l_{ee} from the PC orifice. In order to numerically estimate the e - e scattering contribution to the PC-resistance in this regime we weight the integral over the dimensionless distance r in (B1) by an exponential factor $\exp(-ar/l_{ee})$, where the T -dependent l_{ee} is taken from the quasiparticle life-time calculations¹⁹. Most probably, this approach can not be justified by a solution of the kinetic equation and should be treated as a first crude step on the way to a self-consistent calculation. Nevertheless, such an account of the beam decay allows to describe the experimental T -dependence in the whole range of temperatures. In fig. 12 we plot the best numerical fits (lines) to the experimental data (symbols) for the 5 lowest values of R_0 used. The data ordinate are shifted in steps of 0.05 for successive R_0 . The saturation of the T -dependence in the range $T > 2\text{K}$ is perfectly reproduced by the fits, which strongly supports our interpretation in terms of the e - e scattering. The overall quality of the fits is pretty good for $R_0 \leq 2.7k\Omega$. At higher R_0 the agreement is worse, presumably thanks to a residual thermal smearing of the conductance plateaus (see section III).

As follows from fig. 11 and fig. 12, a cut-off length on the order of $l_c \sim 10\mu\text{m}$ is too small to clearly observe the proportionality¹³ $\delta G_{ee} \propto T$. Improving the sample quality one could achieve longer elastic mean-free path (and l_c), which favors linearity of the T -dependence at temperatures such that $T/E_F \gg a/l_c$ (see fig. 11

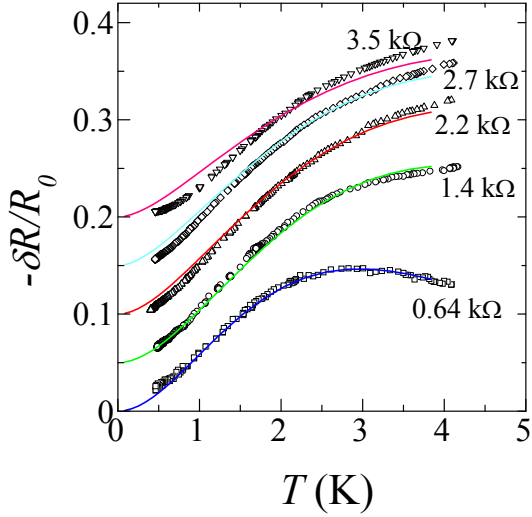


FIG. 12. Normalized experimental T -dependence of the PC-resistance (symbols) together with numerical fits accounting for the beam decay effect (lines), shifted in steps of 0.05 along the ordinate axis for clarity. These fits are obtained with the cut-off length equal to $l_c = 8.5\mu\text{m}$ for $R_0 = 0.64\text{k}\Omega$ and $l_c = 5\mu\text{m}$ for the four other curves. The parameter a equals twice the physical half-width of the PC orifice from fig. 7 (dots). The e - e interaction parameter values are given in fig. 9 (circles).

and discussion in section VIA). On the other hand, the beam decay effect could not be neglected unless $l_c \ll l_{ee}$, which is harder to satisfy at higher l_c . The trade-off is to increase l_c and measure at lower temperatures in order to satisfy simultaneously $a(T/E_F)^{-1} \ll l_c \ll l_{ee} \propto (T/E_F)^{-2}/\ln(E_F/T)$. These conditions are possible, yet challenging to meet, and is simpler to do in higher density (large E_F) samples. For a GaAs, we expect that a T -dependence close to $\delta G_{ee} \propto T$ could be observed at $0.1\text{K} < T < 1\text{K}$ in samples with a 2DES mobility exceeding $10^7\text{cm}^2/\text{Vs}$.

-
- ¹ Yu. V. Sharvin, Zh. Eksp. Teor. Fiz. **48**, 984 (1965) [Sov. Phys. JETP **21**, 655 (1965)]; Yu. V. Sharvin and N. I. Bogatina, Zh. Eksp. Teor. Phys. **56**, 772 (1969) [Sov. Phys. JETP **29**, 419 (1969)].
- ² L.I. Glazman, G.B. Lesovik, D.E. Khmelnitskii, R.I. Shekhter, JETP LETTERS **48**, 238 (1988).
- ³ B.J. van Wees, H. van Houten, C.W.J. Beenakker, et al., Phys.Rev.Lett. **60**, 848 (1988).
- ⁴ D.A.Wharam, T.J.Thornton, R.Newbury, et al., J. Phys. C: Solid State Phys. **21**, L209 (1988).
- ⁵ P.F. Bagwell, P.T. Orlando, Phys. Rev. B **40**, 1456 (1989).
- ⁶ B.J. van Wees, L.P. Kouwenhoven, E.M.M. Willems, C.J.P.M. Harmans, J.E. Mooij H. van Houten, C.W.J. Beenakker, J.G. Williamson, C. T. Foxon, Phys. Rev. B **43**, 12431 (1991).
- ⁷ K.J. Thomas, J.T. Nicholls, M.Y. Simmons, M. Pepper, D.R. Mace, D.A. Ritchie, Phys. Rev. Lett. **77**, 135 (1996).
- ⁸ L.W. Molenkamp and M.J.M. de Jong, Phys. Rev. B **49**, 5038 (1994); M.J.M. de Jong and L.W. Molenkamp, *ibid.* **51**, 13389 (1995).
- ⁹ R.N. Gurzhi, A.N. Kalinenko, A.I. Kopeliovich, Phys. Rev. Lett. **74**, 3872 (1995).
- ¹⁰ A.O.Govorov and J.J.Heremans, Phys. Rev. Lett. **92**, 026803 (2004).
- ¹¹ D. Taubert, G.J. Schinner, H.P. Tranitz, W. Wegscheider, C. Tomaras, S. Kehrein, S. Ludwig, Phys. Rev. B **82**, 161416(R) (2010); D. Taubert, C. Tomaras, G.J. Schinner, H.P. Tranitz, W. Wegscheider, S. Kehrein, S. Ludwig, *ibid.* **83**, 235404 (2011).
- ¹² V.T. Renard, O. A. Tkachenko, V. A. Tkachenko, et al., Phys. Rev. Lett. **100**, 186801 (2008).
- ¹³ K.E. Nagaev and O.S. Ayvazyan, Phys.Rev.Lett. **101**, 216807 (2008).
- ¹⁴ K.E. Nagaev, T.V. Kostyuchenko, Phys.Rev.B **81**, 125316 (2010).
- ¹⁵ K.E. Nagaev, T.V. Krishtop, N.Yu. Sergeeva, Pis'ma v ZhETF, **94**, 53 (2011).
- ¹⁶ Examples of conductance quantization in one of our devices are given in Fig. 1 of the supplementary material.
- ¹⁷ This behavior in magnetic fields is in stark contrast with that of a well-known weak-localization (WL) correction in diffusive 2D and quasi-1D systems. In those systems, the low- B magnetoresistance is (i) negative and (ii) strengthens at decreasing T (see, e.g., Ref.¹⁸ and Ref.²² for a review), which is opposite to our observations. Obviously, the WL physics is not important in clean ballistic PCs we study here.
- ¹⁸ K.K. Choi, D.C. Tsui, K. Alavi, Phys. Rev. B **36**, 7751 (1987).
- ¹⁹ G.F. Giuliani, J.J. Quinn, Phys. Rev. B **26**, 4421 (1982).
- ²⁰ B.J. LeRoy, J.Phys.: Condens. Matt. **15**, R1835 (2003).
- ²¹ H. van Houten, C. W. J. Beenakker, P. H. M. Loosdrecht, et al., Phys. Rev. B **37**, 8534 (1988).
- ²² C. W. J. Beenakker, H. van Houten, Solid State Physics, **44**, 1-228 (1991).
- ²³ F. Stern, Phys. Rev. Lett. **18**, 546 (1967).
- ²⁴ D.S. Saraga, B.L. Altshuler, D. Loss, R.M. Westervelt, Phys. Rev. B **71**, 045338 (2005).
- ²⁵ At $T \rightarrow 0$ we expect instead of eq. (2) a simpler relation $\delta G_{ee}/G_0 \sim l_c/l_{ee}^* \ll 1$, where $l_{ee}^* \propto T^{-2}$ is a mean free path

for e - e scattering in the 2DES, determined by large-angle scattering⁹. Note, however, that in this limit the notion of the cutoff length l_c may be incorrect (K.E. Nagaev, private communication).

²⁶ L.W. Molenkamp, A.A.M. Staring, C.W.J. Beenakker, R. Eppenga, C.E. Timmering, J.G. Williamson, C.J.P.M. Harmans, C.T. Foxon, Phys. Rev. B **41**, 1274 (1990).

²⁷ U. Sivan, M. Heiblum, C.P. Umbach, H. Shtrikman, Phys. Rev. B **41**, 7937 (1990).

²⁸ J. Spector, H.L. Stormer, K.W. Baldwin, L.N. Pfeiffer, K.W. West, Appl. Phys. Lett. **56**, 1290 (1990).

²⁹ D.A. Wharam, U. Ekenberg, M. Pepper, D.G. Hasko, H. Ahmed, J.E.F. Frost, D.A. Ritchie, D.C. Peacock, and G.A.C. Jones, Phys. Rev. B **39**, 6283 (1989).

Supplementary material

M. Yu. Melnikov,¹ J.P. Kotthaus,² V. Pellegrini,³ L. Sorba,³ G. Biasiol,⁴ and V.S. Khrapai¹

¹*Institute of Solid State Physics, Russian Academy of Sciences, 142432 Chernogolovka, Russian Federation*

²*Center for NanoScience and Fakultät für Physik, Ludwig-Maximilians-Universität,
Geschwister-Scholl-Platz 1, D-80539 München, Germany*

³*NEST, Istituto Nanoscienze-CNR and Scuola Normale Superiore, Piazza San Silvestro 12, I-56127 Pisa, Italy*

⁴*CNR-IOM, Laboratorio TASC, Area Science Park, I-34149 Trieste, Italy*

I. LOW TEMPERATURE CONDUCTANCE QUANTIZATION

We study the e - e scattering contribution to the point-contact (PC) resistance at temperatures above $T \approx 0.5\text{K}$. As shown in fig. 1 of the main paper, the resistance quantization is rather poor, which we interpret as a result thermal smearing of the Fermi distribution function¹. In order to demonstrate this, we cool one of the samples down to $T \approx 60\text{mK}$ and observe clearly quantized conductance plateaus, see fig. 1. Such a quality of quantized PC conductance is routinely observed in our devices at low- T and rules out disorder as origin of the poor quantization at higher temperatures.

II. R_0 AT ELEVATED TEMPERATURES

As discussed in the main paper, a direct extrapolation of the T -dependence $R(T)$ towards a zero temperature

limit (R_0) is problematic. One way to determine R_0 is from a magnetoresistance data in small magnetic fields at the lowest T , where the e - e scattering contribution is almost absent. However, this procedure is not applicable at $T \geq 1\text{K}$, where magnetoresistance is not of purely single-particle origin. Unfortunately, resistance drifts on the order of $\pm 2\%$ prevent using the lowest- T value of R_0 at a given gate-voltage. Instead, when scaling the magnetoresistance data, we allow a variation of R_0 by a few percent at a given T and V_g . In fig. 2, the R_0 values used for scaling in fig. 6b of the main paper (symbols) are plotted along with the measured gate-voltage dependencies of the PC-resistance for a set of temperatures studied (lines). The R_0 data points exhibit scatter at different T and fall close to the lowest temperature trace $R(V_g)$, except for some points at $T = 4.2\text{K}$.

¹ P.F. Bagwell, P.T. Orlando, Phys. Rev. B **40**, 1456 (1989).

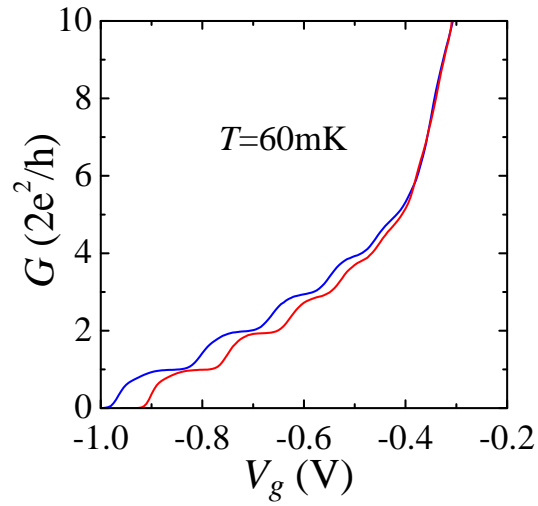


FIG. 1. Gate-voltage dependence of a linear-response PC-conductance in one of the samples studied in the main paper (two different constrictions). The data are taken in a dilution $^3\text{He}/^4\text{He}$ refrigerator with a 60mK base temperature.

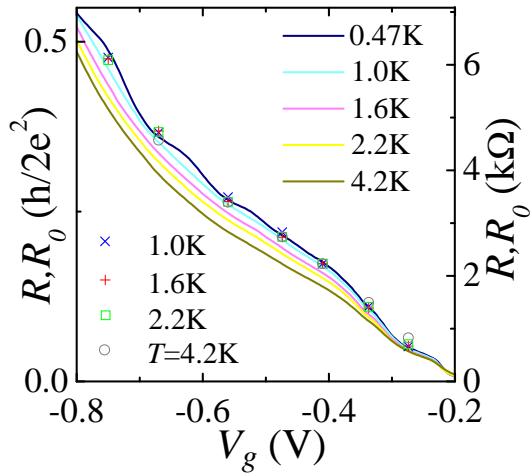


FIG. 2. Gate-voltage dependence of the PC-resistance for a set of temperatures used in experiment (lines, see legend). Symbols mark the values of R_0 used for scaling of the magnetoresistance data in fig. 6b of the main paper at temperatures $T \geq 1\text{K}$ (see legend).